Available online at www.sciencedirect.com
ScienceDirect
Journal of the European Ceramic Society 26 (2006) 3315–3324
www.elsevier.com/locate/jeurceramsoc

Transport properties of sealants for high-temperature electrochemical applications: RO–BaO–SiO_2 (R = Mg, Zn) glass–ceramics

M.J. Pascual [a,*], V.V. Kharton [b], E. Tsipis [b], A.A. Yaremchenko [b], C. Lara [a], A. Durán [a], J.R. Frade [b]

[a] *Ceramics and Glass Institute, CSIC, Campus of Cantoblanco, 28049 Madrid, Spain*
[b] *Department of Ceramics and Glass Engineering, CICECO, University of Aveiro, 3810-193 Aveiro, Portugal*

Received 19 August 2005; received in revised form 26 October 2005; accepted 6 November 2005
Available online 13 December 2005

Abstract

The electrical properties and oxygen permeability of glass–ceramics $55SiO_2$–27BaO–18MgO, $55SiO_2$–27BaO–18ZnO and $50SiO_2$–30BaO–20ZnO (%mol), which possess thermal expansion compatible with that of yttria-stabilized zirconia (YSZ) solid electrolytes, were studied between 600 and 950 °C in various atmospheres. The ion transference numbers, determined by the modified electromotive force (e.m.f.) technique under oxygen partial pressure gradients of 21 kPa/(1–8) × 10^2 Pa and 21 kPa/(1 × 10^{-18}–2 × 10^{-12}) Pa, are close to unity both under oxidizing and reducing conditions. The electronic contribution to the total conductivity increases slightly on increasing temperature, but is lower than 2% and 7% for the Zn- and Mg-containing compositions, respectively. The conductivity values measured by impedance spectroscopy vary in the range (1.4–7.8) × 10^{-6} S/cm at 950 °C under both oxidizing and reducing conditions, with activation energies of 122–154 kJ/mol and a minor increase in H_2-containing atmospheres, indicating possible proton intercalation. In agreement with the electrical measurements which indicate rather insulating properties of the glass–ceramics, the oxygen permeation fluxes through sintered sealants and through sealed YSZ/glass–ceramics/YSZ cells are very low, in spite of an increase of 15–40% during 200–230 h under a gradient of air/H_2–H_2O–N_2 due to slow microstructural changes.

Keywords: Electrical properties; Ionic conductivity; Glass ceramics; Fuel cells; Sealants

1. Introduction

One important challenge in the development of planar solid oxide fuel cells (SOFCs) relates to the development of suitable sealant materials to separate the cathode and anode chambers, and to maintain gas-tightness of the system at elevated temperatures, 600–1000 °C.[1–3] Seals are applied to the cell edges between interconnect and electrolyte and/or electrodes, depending on the system design, and also to the gas manifolds to bond them to the sintered electro-active components. The key requirements for sealing materials include thermomechanical and chemical stability, negligible physical and electrochemical leakages throughout the range of the SOFC operation conditions, and thermal expansion coefficients (TECs) similar to those of other cell components, (9–13) × 10^{-6} K^{-1}.[4–6] The seal should also behave as an electrical insulator, with total conductivity (σ) lower than 10^{-4} S/cm, in order to avoid parasitic currents decreasing the system efficiency. Finally, a good chemical compatibility with all the other SOFC materials, in particular interconnect alloy and solid electrolyte, is necessary.[4–7]

Several approaches have been used to achieve the required adherence, mechanical integrity and stability, including both rigid[7–13] and compressive[14–17] seals. The most common approach is to use rigid glass or glass/ceramic seals, where no load should be applied during operation. However, as these materials are inherently brittle, a number of metallic, metallic–ceramic and ceramic–ceramic composite seals have been developed, both in rigid and in compressive configurations. The use of multiphase sealants makes it possible to

* Corresponding author. Tel.: +34 91 7355840; fax: +34 91 7355843.
E-mail address: mpascual@icv.csic.es (M.J. Pascual).

0955-2219/$ – see front matter © 2005 Elsevier Ltd. All rights reserved.
doi:10.1016/j.jeurceramsoc.2005.11.002

improve wettability, compliance at interfaces and strain relief, gas-tightness and stability.

A promising combination of physicochemical properties were found in the systems RO–BaO–SiO_2 where R = Mg and Zn,[5,12,13] including suitable dilatometric characteristics and sintering/crystallization behaviour which resulted in dense materials with the desired microstructure at temperatures around 850 °C. For these glass–ceramics, sealing of planar SOFCs may be performed at 700–800 °C via sintering of the glass powder during start-up; further treatment at the operation temperature induces the precipitation of crystalline phases which generate a rigid seal with good thermal, chemical and mechanical stability.[13] Impedance spectroscopy studies in air showed that these materials behave as insulators in the entire temperature range relevant for SOFCs, 500–1000 °C.[18] The present work continues electrical and electrochemical characterization of the glass–ceramic sealants selected in the RO–BaO–SiO_2 systems, with special emphasis on oxygen permeability and conductivity in various atmospheres, properties which are of key importance for practical applications. Another goal was to evaluate the applicability of the electromotive force (e.m.f.) technique and oxygen permeation measurements for the assessment of ion-transport parameters in Si-containing glass–ceramics. Although the e.m.f. method is widely used to determine ionic and electronic contributions to the total conductivity of ceramic solid oxide electrolytes and mixed conductors,[19–21] the study of glass-based materials is complicated due to numerous factors, such as fast surface diffusion of silica, stagnated interfacial exchange and high electrical resistivity.

2. Experimental

2.1. Materials preparation and characterization

The chemical compositions and corresponding abbreviations of glass–ceramics studied in the present work are listed in Table 1. For all materials, the BaO/RO (R = Mg or Zn) ratio was kept maintained at 1.5. Batch compositions (75 g of each) were prepared using reagent-grade $BaCO_3$, $MgCO_3$, ZnO, and SiO_2 sand containing <30 ppm of Fe_2O_3. The raw materials were thoroughly mixed and melted in a Pt crucible at 1650 °C for 2 h, casted on brass moulds and annealed around the glass transition temperature (T_g). The detailed physicochemical characterization of the glasses using dilatometry, hot-stage microscopy (HSM) and differential thermal analysis (DTA) was reported previously;[13] selected data are summarised in Table 2.

Table 1
Glass compositions and abbreviations

Abbreviation	Composition (mol%)			
	SiO_2	BaO	MgO	ZnO
Mg1.5-55	55	27	18	–
Zn1.5-55	55	27	–	18
Zn1.5-50	50	30	–	20

For preparation of gas-tight glass–ceramics, powdered glasses with particle size less than 20 μm (d_{50} = 10 μm) were pressed uniaxially into pellets (18 mm diameter, ~2 mm thickness, relative density of 64%) at approximately 100 MPa. The subsequent thermal treatment included heating to 900 °C (5 °C/min), sintering at 900 °C for 0.5 h, cooling to 850 °C (5 °C/min) with annealing at 850 °C for 1 h, and, finally, cooling down to room temperature (2 °C/min). The density of sintered glass–ceramics was 90% relative to the density of the bulk glass composition. All samples were checked for gas-tightness by the absence of gas leakage through samples placed under a pressure gradient of 2–3 atm at room temperature. The phase composition of the glass–ceramics was analysed by X-ray diffraction (XRD) using a Siemens D5000 instrument. The microstructure was studied by scanning electron microscopy (SEM) coupled with energy dispersive spectroscopy (EDS), using a Hitachi S-4100 microscope and a Rontec UHV detection system.

The total conductivity was studied by AC impedance spectroscopy (HP4284A precision LCR meter, 20 Hz–1 MHz), using dense pelletised samples with Pt electrodes. Measurements were performed in temperature range 600–950 °C in flowing air, Ar, 10% H_2–90% N_2, and various H_2–H_2O–N_2 mixtures, and also as function of time at 850–950 °C in a 10% H_2–90% N_2 gas flow. The oxygen partial pressure in the measuring chamber was determined with an yttria-stabilized zirconia (YSZ) electrochemical sensor.

2.2. Modified e.m.f. technique

The e.m.f. technique used to determine ion transference numbers of the glass–ceramic materials is based on the

Table 2
Dilatometric, HSM and DTA data for the studied glasses

Property	Technique	Composition		
		Mg1.5-55	Zn1.5-55	Zn1.5-50
Average thermal expansion coefficient ($\bar{\alpha} \pm 0.5$) × 10^6 K^{-1} (50–500 °C)	Dilatometry	10.0	9.2	10.4
Glass transition temperature $T_g \pm 3$ (°C)	Dilatometry	711	655	666
Dilatometric softening temperature $T_d \pm 5$ (°C)	Dilatometry	750	702	708
First shrinkage temperature $T_{FS} \pm 5$ (°C)	HSM	750	700	717
Maximum shrinkage temperature $T_{MS} \pm 5$ (°C)	HSM	824	780	785
Onset crystallization temperature $T_X \pm 2$ (°C)	DTA	852	837	830
Crystallization temperature $T_C \pm 2$ (°C)	DTA	877	857	854
Half ball temperature $T_{half\ ball} \pm 5$ (°C)	HSM	1175	1120	1140
Flow temperature $T_{flow} \pm 5$ (°C)	HSM	1200	1125	1150

measurement of the open-circuit voltage of a cell consisting of a membrane with two electrodes, placed under a chemical potential gradient.[19–21] For an oxide sample with negligible electrode polarization resistance tested in an oxygen concentration cell, the average ion transference number (t_i) within the given oxygen pressure gradient can be obtained from the ratio of measured e.m.f. (E_{obs}) and theoretical Nernst voltage (E_{th}):

$$t_i = \frac{E_{obs}}{E_{th}} = E_{obs}\left[\frac{RT}{4F}\ln\frac{p_2}{p_1}\right]^{-1} = \frac{\sigma_i}{\sigma_i + \sigma_e} = \frac{R_e}{R_e + R_i} \quad (1)$$

where p_1 and p_2 are the values of oxygen partial pressure at the electrodes, σ_i and σ_e are the partial ionic and electronic conductivities, and R_i and R_e are the partial ionic and electronic resistances of the membrane, respectively. Non-negligible electrode polarisation leads to an underestimation of t_i; the relation between apparent (t_i^{obs}) and true ion transference numbers is expressed as:[20–22]

$$t_i^{obs} = \frac{E_{obs}}{E_{th}} = t_i\left(1 + \frac{R_\eta}{R_i + R_e}\right)^{-1} \quad (2)$$

where R_η, is the electrode polarisation resistance. For glass–ceramic samples, this situation is very likely due to low exchange currents and surface diffusion of silica, which may block the porous Pt electrodes. In order to take electrode polarisation into account, Gorelov's modification of the e.m.f. method[21,22] was used. This modification is based on the measurement of cell voltage as a function of an external load resistance (R_M), when

$$\frac{E_{th}}{E_{obs}} - 1 = (R_i + R_\eta)\left[\frac{1}{R_e} + \frac{1}{R_M}\right] \quad (3)$$

The true ion transference numbers can be calculated from the results of AC impedance spectroscopy and the values of R_e

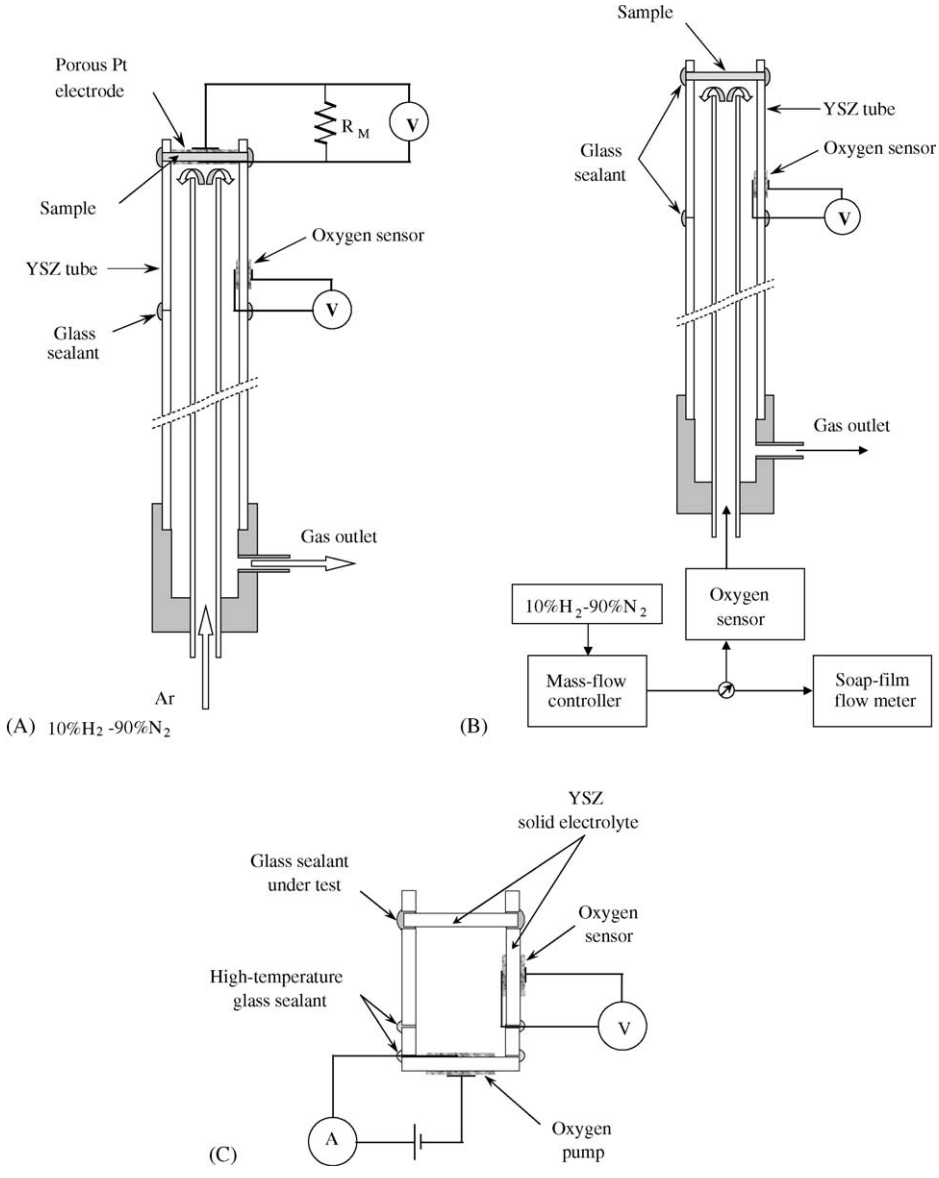

Fig. 1. Schematic drawings of the experimental setups for the modified e.m.f. technique (A), oxygen permeation measurements (B), and YSZ sealing tests (C).

obtained from a simple regression of the linear part of a plot of $(E_{th}/E_{obs} - 1)$ versus $1/R_M$:

$$\frac{E_{th}}{E_{obs}} - 1 = A\left(\frac{1}{R_M}\right) + B; \quad R_e = \frac{A}{B} \tag{4}$$

$$t_i = 1 - \frac{R_{bulk}}{R_e} \tag{5}$$

where A and B are regression parameters, and R_{bulk} is the bulk resistance determined from the impedance spectra.

The experimental cell for e.m.f. measurements comprised a glass–ceramic membrane (0.65 mm thickness, 12.5 mm diameter) with porous Pt electrodes, hermetically sealed onto YSZ tube using a Pyrex glass (Fig. 1A). The 10% H_2–90% N_2 or O_2–Ar mixtures were supplied at the inner electrode, where the oxygen partial pressure (p_1) was determined using a YSZ sensor; the outer electrode was exposed to atmospheric air ($p_2 = 21$ kPa). The e.m.f. of the cell was measured at 700–950 °C as a function of an external resistance, R_M. The ion transference numbers were calculated using regression model Eq. (4) in combination with Eq. (5), as illustrated by Fig. 2.

2.3. Oxygen permeation

The measurement technique used for the determination of oxygen permeation fluxes through glass–ceramics under air/H_2–H_2O gradients typical for SOFC operation is based on the analysis of oxygen activity in the gas flow over the sample permeate side. The experimental setup (Fig. 1B) comprises a dense membrane disk (0.65 mm thickness) hermetically sealed onto an YSZ tube, and two oxygen sensors at the inlet and outlet of the cell. A flow of H_2–H_2O–N_2 gas mixture (10.3 cm^3/min) was supplied to the membrane permeate side, where hydrogen interacted with oxygen permeating through the glass–ceramics. The gas flow rate (V) was controlled with Bronkhorst mass-flow controllers and additionally measured at the outlet by a soap-film flow meter. For the e.m.f. measurements, the membrane feed side was exposed to atmospheric air ($p_2 = 21$ kPa). The oxygen permeation flux density (j) through a membrane under steady-state conditions was calculated as:

$$j = \frac{V}{RT_V S}\frac{p(H_2)_{in} - p(H_2)_{out}}{2} \tag{6}$$

where T_V is the flow meter temperature, S the membrane surface area, and $p(H_2)_{in}$ and $p(H_2)_{out}$ are the hydrogen partial pressures at the inlet and outlet of the measuring cell, respectively. The hydrogen pressure was calculated by

$$p(H_2) = \frac{CP_{total}}{1 + K \times p(O_2)^{1/2}} \tag{7}$$

where C is the volume fraction of H-containing species ($H_2 + H_2O$) in the gas determined by its initial composition, P_{total} the total pressure, K the equilibrium constant of the H_2 oxidation reaction calculated using thermodynamic data,[23] and $p(O_2)$ the oxygen partial pressure in the gas flow determined by the oxygen sensor. The accuracy of the measurement technique was verified sealing a thick (3–4 mm) YSZ disk with porous Pt electrodes instead of the glass–ceramic membrane and pumping various amounts of oxygen in the gas flow; the errors in the oxygen flux determination varied in the range 0.1–5%, decreasing with increasing oxygen flux. These errors are primarily caused by minor physical and electrolytic leakages into the system and parasitic thermo-e.m.f. of the oxygen sensors. If compared to the oxygen permeation fluxes reported below, the overall leakages estimated under conditions when no oxygen was pumped into the system, were lower than 3%.

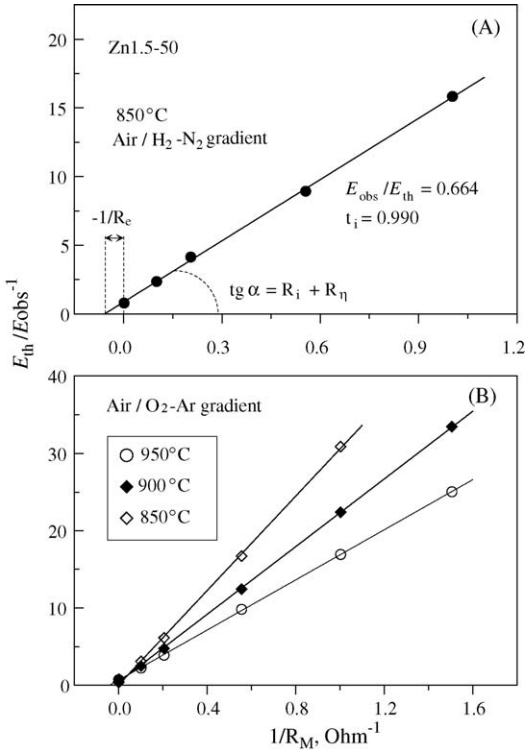

Fig. 2. Determination of the ion transference numbers by the modified e.m.f. technique, for the example of Zn1.5-50 glass–ceramics. Solid lines correspond to the fitting results, using Eq. (6) as the linear regression model.

2.4. Sealing tests

The sealing tests of YSZ ceramics, performed to assess electrochemical leaks through the YSZ/glass–ceramics/YSZ interfaces, were carried out using Zn1.5-50 glass powder. As shown by the impedance spectroscopy and e.m.f. measurement results discussed below, this composition possesses the lowest total and partial electronic conductivities with respect to the other studied sealants, and is, thus, the most promising for practical applications. The electrochemical cells used for the sealing tests (Fig. 1C) are made of YSZ solid electrolyte (2.0 mm wall thickness) and comprise an oxygen sensor and an oxygen pump with porous Pt electrodes; Pt wires are used as current collectors. All cell components, except for a YSZ membrane at the top, were assembled and sealed at 1280–1320 °C using another sealant based on the SiO_2–CaO–BaO–Al_2O_3 system; physicochemical and transport properties of the high-temperature sealants will be reported in subsequent parts of this work. Under the measurement conditions, the oxygen permeability of the

high-temperature sealant was found below the detectable limit. After fabrication, the electrochemical cells were tested for gas-tightness. The YSZ membrane (2 mm thickness) was then sealed onto the top using the Zn1.5-50 glass powder; the thermal treatment procedure in the course of sealing involved heating to 1100–1150 °C (2 °C/min) in air, sealing at temperatures close to the half-ball temperature (Table 2) for 5–15 min, and cooling down to the measurement temperature, 850–950 °C. In the course of sealant assessment, oxygen was pumped out of the cell by passing a direct current through the oxygen pump until the required $p(O_2)$ value was obtained; the current was then switched off and the oxygen leakage was monitored by measuring the oxygen partial pressure inside the cell as a function of time. After the experiments, YSZ/glass–ceramics/YSZ interfaces were inspected by SEM/EDS.

3. Results and discussion

3.1. Transference numbers

The e.m.f. measurements confirmed that, as expected, the role of electrode polarization resistance in the oxygen concentration cells with glass–ceramic membranes is essential, making it impossible to determine the ion transference numbers simply from the measured voltage using Eq. (1). As an example, Fig. 3 compares the ratio of measured and theoretical voltages (E_{obs}/E_{th}) and the true values of ion transference numbers determined by the modified e.m.f. technique, for composition Zn1.5-50. The t_i^{obs} values vary in the range 0.5–0.8, while the ionic contribution to total conductivity of the glass–ceramics is close to 100%. Note that predominant ionic conduction was also confirmed by the impedance spectra, which consist of two arcs corresponding to the bulk and electrode signals (Fig. 4).

Table 3 summarises the ion transference numbers of Mg1.5-55 and Zn1.5-50 glass–ceramics. As the differences in the composition and physicochemical properties of Zn1.5-50 and Zn1.5-55 are very minor (Tables 1 and 2), the transference numbers of the latter material are expected very similar to those of Zn1.5-50. In oxidizing atmospheres, the values of t_i vary in the

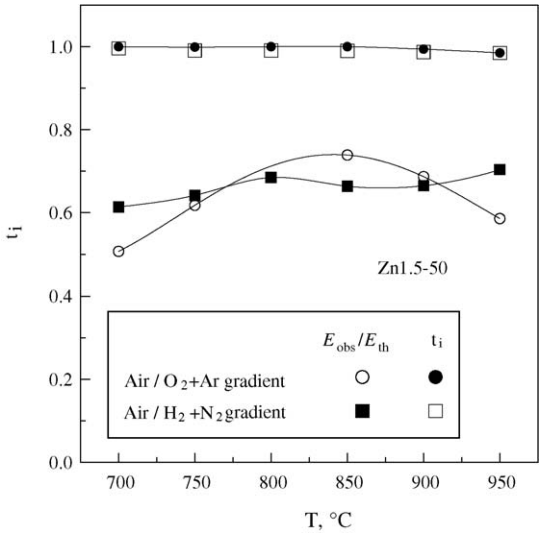

Fig. 3. Comparison of the ion-transference numbers and the ratio between observed and theoretical e.m.f. values for the Zn1.5-50 glass–ceramics with Pt electrodes. The corresponding values of oxygen partial pressure in the gas mixtures supplied to the electrodes are given in Table 3.

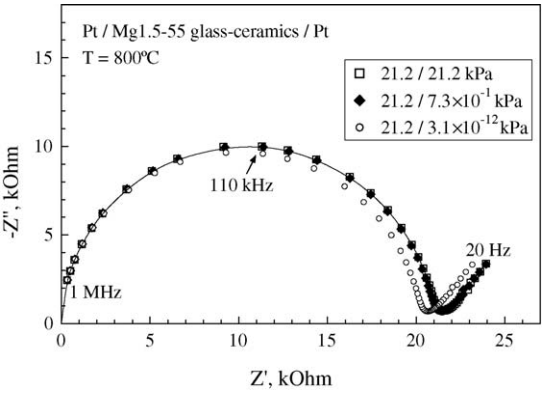

Fig. 4. Typical impedance spectra of Mg1.5-55 glass–ceramics with porous Pt electrodes at 800 °C under various $p(O_2)$ gradients, indicated in the legend.

Table 3
Oxygen transference numbers determined by the modified e.m.f. technique

Composition	T (°C)	Air/O_2–Ar gradient		Air/10% H_2–90% N_2 gradient	
		p_1 (Pa)	t_i	p_1 (Pa)	t_i
Zn1.5-50	950	110 ± 3	0.985 ± 0.004	1.7×10^{-13}	0.985 ± 0.002
	900		0.994 ± 0.004	2.7×10^{-14}	0.987 ± 0.004
	850		1.000 ± 0.007	2.3×10^{-15}	0.990 ± 0.004
	800		1.000 ± 0.002	3.9×10^{-16}	0.991 ± 0.005
	750		0.999 ± 0.008	4.5×10^{-17}	0.991 ± 0.006
	700		1.000 ± 0.009	9.5×10^{-19}	0.996 ± 0.006
Mg1.5-55	950	760 ± 40	0.95 ± 0.01	2.2×10^{-12}	0.93 ± 0.03
	900		0.97 ± 0.06	2.6×10^{-13}	0.93 ± 0.03
	850		–	3.0×10^{-14}	0.94 ± 0.08
	800		0.97 ± 0.09	3.1×10^{-15}	0.95 ± 0.02
	750		–	2.9×10^{-16}	0.97 ± 0.01
	700		–	2.9×10^{-17}	0.97 ± 0.08

Note: p_2 is equal to 21 kPa (atmospheric air). The errors are given for a confidence interval of 95%.

range 0.95–1.00 whereas that of Zn1.5-50 is higher than that of Mg1.5-50. The electronic contribution increases with increasing temperature, indicating that the activation energy for the ionic transport is lower than that of electronic transport. Similar behaviour is known for Si-containing crystalline phases without transition metal oxide dopants, such as oxygen ion-conducting La_{10-x} (Si, Al)$_6$ $O_{27-\delta}$ apatites.[24] Under large $p(O_2)$ gradients typical for SOFC operation, the electron transference numbers are slightly higher, but still lower than 2% and 7% for the Zn- and Mg-containing compositions, respectively.

Inspection of the samples by SEM/EDS revealed no essential microstructural changes in the membrane bulk after the e.m.f. measurements (Fig. 5A and B, top view). The high surface diffusivity of silica results in substantial conglutination of Pt particles forming the electrodes (Fig. 5C and D, fracture surface). This phenomenon is one of the most likely reasons for the significant polarisation effects; another may relate to stagnated oxygen exchange between the glassy and gas phases. Nonetheless, the porosity of the electrode layers is still sufficient and the triple gas/Pt/glass–ceramics boundaries providing electrochemical reaction sites still exist. One should also mention a moderate interaction between the glass–ceramics and Pyrex glass used for sealing; one typical SEM micrograph is given in Fig. 5E. EDS analysis showed that a small amount of NaO diffuses into the glass–ceramics up to a depth of 10–20 μm from the interface. It seems, very unlikely however, that these phenomena could lead to significant parasitic electronic conducting in the oxygen concentration cells.

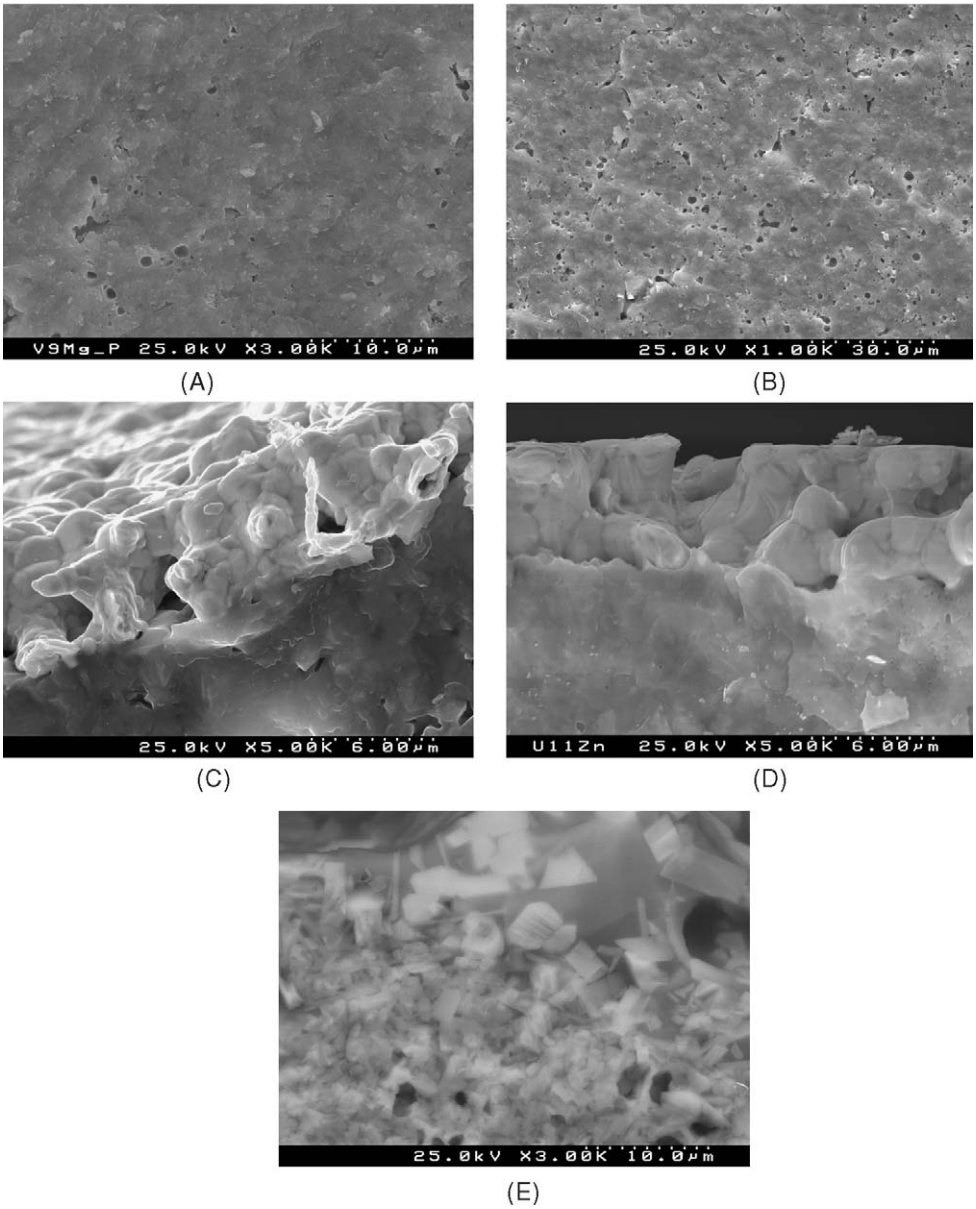

Fig. 5. SEM micrographs of fractured Mg1.5-55 (A–C) and Zn1.5-50 (D and E) glass–ceramics: as-prepared sample (A), glass–ceramics after the e.m.f. measurements (B), glass–ceramic/Pt interfaces (C and D), and glass–ceramic/Pyrex interface (E). For (C–E), Pt and Pyrex layers are at the top of the micrographs.

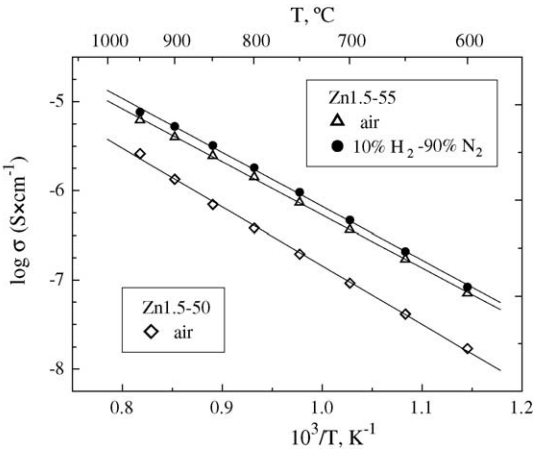

Fig. 6. Total conductivity vs. temperature of Zn-containing glass–ceramics in oxidizing and reducing atmospheres.

3.2. Conductivity

The results of total conductivity (σ), summarized in Figs. 6–9, clearly show that the title materials possess good insulating properties within the whole range of SOFC operation conditions. At 950 °C, the conductivity values are in the range $(1.4–7.8) \times 10^{-6}$ S/cm. A slight increase in the conductivity is observed in H_2-containing atmospheres (Figs. 6 and 8), indicating possible proton absorption. On the other hand, the measurements in wet hydrogen with up to 40% water vapour demonstrated that protonic transport only becomes significant at temperatures below 500 °C. The activation energies for the total conductivity, 122–154 kJ/mol, are almost independent of the oxygen chemical potential at 600–950 °C (Table 4).

No degradation of the conductivity with time was found at 850 °C (Figs. 7 and 9). However, annealing in H_2-containing gas mixtures results in a minor increase of electrical resistance; the conductivity at 950 °C varies during 100 h by about 20% for Mg- and 7% for Zn-containing compositions.

It should be emphasized that e.m.f. measurements cannot indicate the exact type of ionic charge carrier(s) when an oxide membrane is placed under an oxygen or metal chemical potential gradient and equilibrium is achieved at the electrodes.[19] The transference numbers listed in Table 3 correspond, therefore, to the total ionic transport, irrespective of the nature of mobile anions and/or cations. The diffusion mechanisms in alkaline-free glasses are still disputable in literature (e.g.[25–28] and references cited), although comparative analysis of the literature data sug-

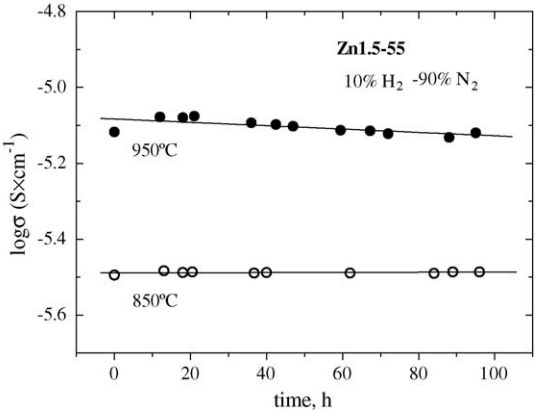

Fig. 7. Time dependence of the total conductivity of Zn1.5-55 glass–ceramics in 10% H_2–90% N_2 atmosphere.

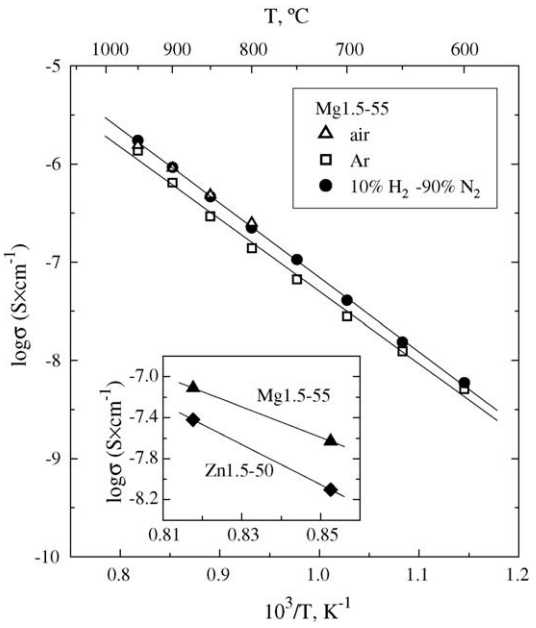

Fig. 8. Total conductivity vs. temperature of Mg1.5-55 glass–ceramics. The inset compares electronic conductivity of glass–ceramic materials under oxidizing conditions.

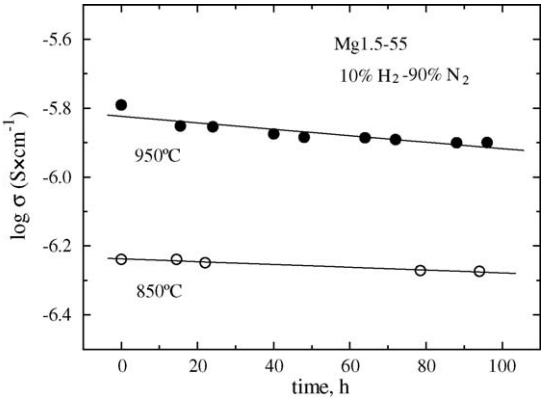

Fig. 9. Time dependence of the total conductivity of Mg1.5-55 glass–ceramics in 10% H_2–90% N_2 atmosphere.

Table 4
Activation energy for the total conductivity at 600–950 °C

Composition	Atmosphere	E_a (kJ/mol)
Zn1.5-55	Air	122 ± 2
	10% H_2–90% N_2	124 ± 4
Zn1.5-50	Air	135 ± 5
Mg1.5-55	Air	143 ± 5
	Ar	149 ± 10
	10% H_2–90% N_2	154 ± 4

gests that anionic conduction in the glasses of RO–BaO–SiO_2 system is often dominating with respect to cationic transport. Furthermore, the properties of glasses are, as a rule, quite similar to those of the parent crystalline phases, as a result of similar bond energetic;[29] numerous SiO_2- and GeO_2-based oxide compounds are known to exhibit predominant oxygen-ionic conductivity.[24,30,31]

Whatever the mechanism of ionic conduction, the level of ionic conductivity in the glass–ceramic sealants seems to be essentially independent on the phase compositions (Fig. 10), and suggest a more important role of microstructural factors. On the contrary, the electronic conductivity appears to correlate with the degree of crystallization and it is higher for Mg1.5-55 glass–ceramics where the XRD analysis indicates a smaller amount of amorphous phase. Such a correlation is reasonable since increasing long-range order should promote electronic band formation. Similar phenomena were observed for other glass–ceramic sealants, which will be reported in the next parts of the present work.

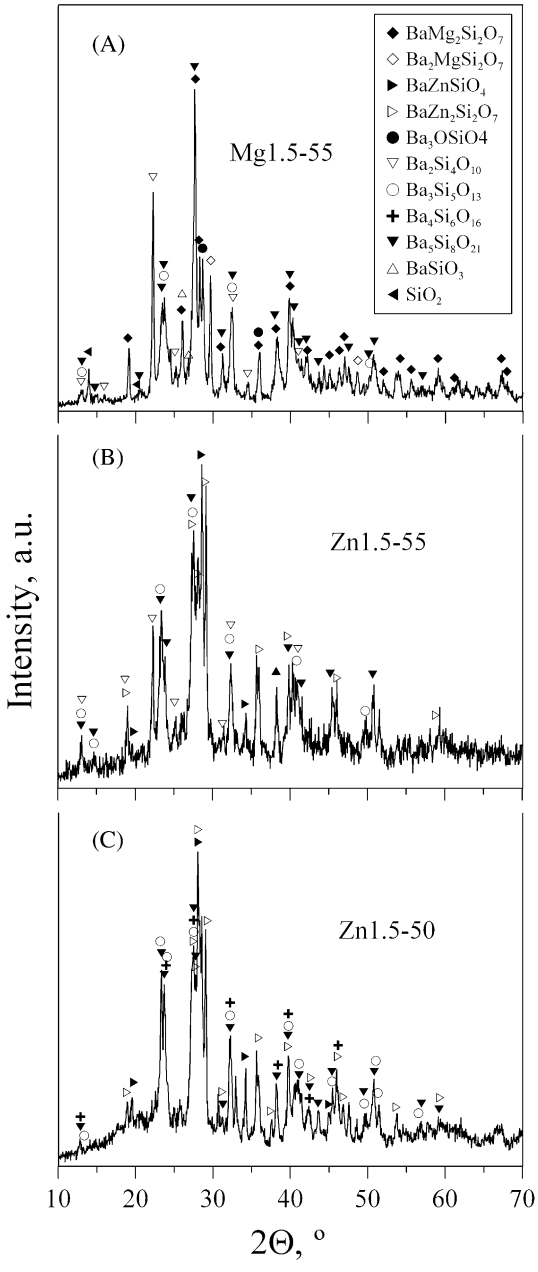

Fig. 10. XRD patterns of glass–ceramic samples after crystallisation.

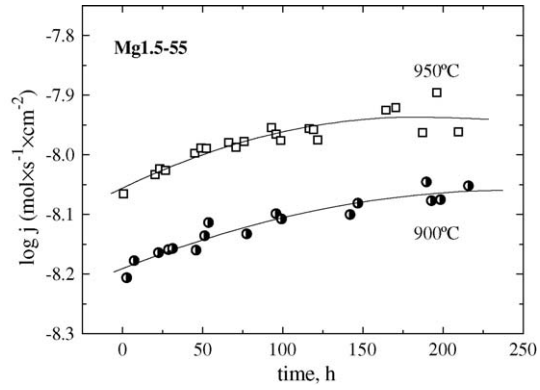

Fig. 11. Time dependence of the oxygen permeation fluxes through Mg1.5-55 glass–ceramic membrane (thickness of 1.0 mm). The feed-side oxygen partial pressure is 21 kPa. The average oxygen partial pressures at the membrane permeate side is 4.9×10^{-15} and 7.6×10^{-15} Pa at 900 and 950 °C, respectively.

3.3. Oxygen permeability

Due to the insulating properties of the title materials, the oxygen permeation fluxes through the glass–ceramic membranes are very low. One example is presented in Fig. 11, showing the permeation fluxes through an Mg1.5-55 sample (thickness, 0.65 mm) under air/H_2–H_2O–N_2 gradient. This level of oxygen permeability is lower than that of La (Ca) $CrO_{3-\delta}$ perovskite ceramics used for SOFC interconnectors.[32]

On the other hand, the permeability undergoes a gradual increase with time. For Mg1.5-55 glass–ceramics tested under an air/H_2–H_2O–N_2 gradient during 200–230 h, the permeation fluxes became 15–40% higher with respect to the initial values (Fig. 11). Subsequent inspection by SEM showed that the degradation may result from microstructural changes, particularly as a result of pore formation near the surface exposed to hydrogen (Fig. 12A). Such behaviour may be associated with SiO volatilization from the surface, which is well known for silicate ceramics (e.g. [24]); this process is thermodynamically favourable and should cause substantial microstructural reconstruction of the near-surface layers. Moreover, the observed values of oxygen permeation fluxes under the air/H_2–H_2O–N_2 gradient are much higher than those predicted theoretically from the data on total conductivity and transference numbers. This suggests a key influence of both surface- and microstructure-related factors, including closed porosity, microcracks and various extended defects. The oxygen fluxes, thus, are expected to rise when the porosity of near-surface layers and/or specific surface area increases. Pore formation and growth is also likely to be responsible for the slow degradation of the total conductivity under reducing conditions (Figs. 7 and 9).

In contrast to the behaviour under air/H_2–H_2O–N_2 gradients, no increase in the permeation fluxes with time was observed in

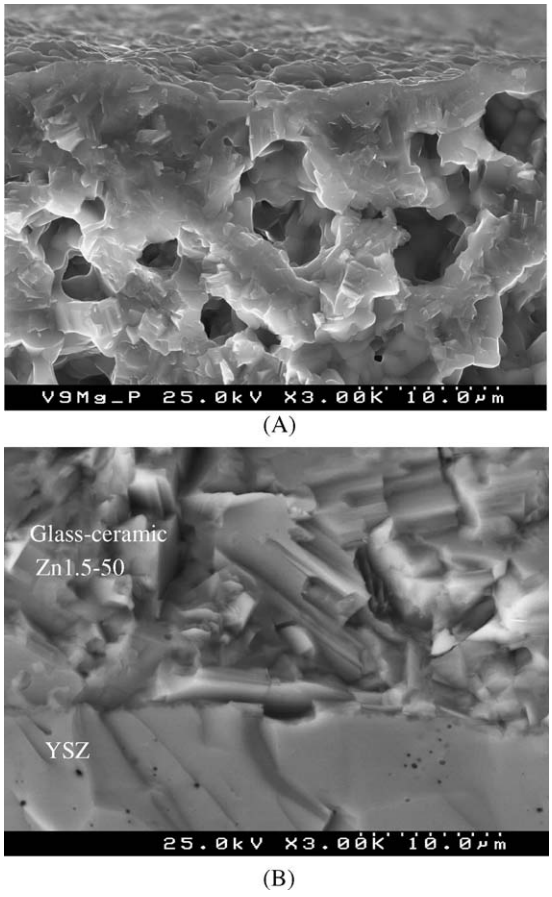

Fig. 12. SEM micrograph of the permeate side of M1.5-55 glass–ceramics fractured after the oxygen permeability measurements (A), and a fractured Zn1.5-50 glass–ceramic/YSZ interface after the sealing test (B).

the course of sealing tests in air. The cells shown in Fig. 1C were hermetically sealed by the Zn1.5-50 glass at 1106–1125 °C; as their hermetisation requires glass flow, the corresponding temperatures were substantially higher compared to those for the planar SOFCs where the sealing procedure requires glass softening and sintering only. The hermetic nature of the sealing was confirmed by pumping oxygen out, which demonstrated that the variations of oxygen partial pressure inside the cell obey Faraday's law. After cooling down to the measurement temperature, 850–950 °C, $p(O_2)$ relaxation curves were collected as a function of time under zero current conditions; representative results are shown in Fig. 13. The oxygen permeation fluxes estimated from these data varied in the range (6–17) $\times 10^{-12}$ mol/s at 950 °C and (8–45) $\times 10^{-13}$ mol/s at 850 °C. This level of permeation is comparable to experimental uncertainties which may be caused by, for example, oxygen desorption from the porous Pt electrodes.[33] Inspection by SEM/EDS revealed the good adherence at the glass–ceramics/YSZ interfaces, absence of cracks, and no reaction between the materials (Fig. 12B).

In summary, the results demonstrate that the modified e.m.f. technique, taking into account the electrode polarisation resistance, can be successfully applied for the determination of ion-transference numbers in glass–ceramics with low conductivity. However, special attention is necessary to avoid block-

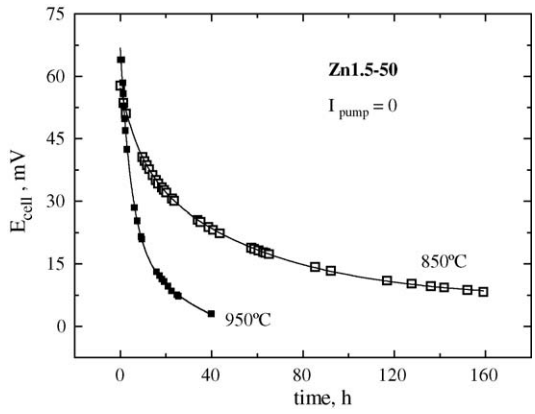

Fig. 13. Time dependence of the sensor e.m.f. through the oxygen pump after switching off the current in the cell shown in Fig. 1C sealed with Zn1.5-50.

ing of porous electrodes by silica, which may occur in the course of long-term experiments. Oxygen permeation fluxes through glass–ceramic membranes are strongly influenced by the microstructure- and surface-related factors, including minor volatilization of silicon oxide. Permeation tests under the SOFC operation conditions are, therefore, necessary to evaluate the performance of sealants, whereas analysis of the oxygen ionic contribution to the total conductivity should be performed by other methods, such as the faradaic efficiency.[21]

4. Conclusions

Glass–ceramics containing 50–55 mol% SiO_2, 27–30% BaO, and 18–20% of MgO or ZnO, were tested as potential SOFC sealants using impedance spectroscopy, determination of ion transference number by the modified e.m.f. technique, and oxygen permeability measurements. At 600–950 °C, the materials exhibit good insulating properties, whilst their conductivity is predominantly ionic. However, a gradual increase in the oxygen permeation flux and a decrease in the conductivity with time are observed when the glass–ceramics are exposed to H_2-containing atmospheres at 900–950 °C. The degradation in reducing conditions is probably associated with volatilization of silicon oxide, which leads to pore formation in the near-surface layers. It is advisable, therefore, to limit the operation temperature to 800–850 °C, and to optimise composition and microstructure of the sealants in order to enhance their stability. The optimisation may be involve the incorporation of submicron particles of stable components such as stabilized zirconia, decreasing total content of SiO_2, and the formation of sandwiched seals where the surface layers prevent diffusion and volatilization of silicon oxide.

Acknowledgements

This work was supported by the Spanish research program MCyT (MAT 2003-0952-C02-01), the OSSEP program (European Science Foundation), and the FCT, Portugal (POCTI program and projects BD/6827/2001 and BPD/11606/2002).

References

1. Steele, B. C. H. and Heinzel, A., Materials for fuel cell technologies. *Nature*, 2001, **414**(6861), 345–352.
2. Singhal, S. C., Solid oxide fuel cells for stationary, mobile, and military applications. *Solid State Ionics*, 2002(152–153), 405–410.
3. Minh, N. Q., Solid oxide fuel cell technology-features and applications. *Solid State Ionics*, 2004, **174**, 271–277.
4. Bieberle, A. and Gauckler, L. J., Glass seals. In *Oxygen Ion and Mixed Conductors and their Technological Applications*, ed. H. L. Tuller, J. Schoonman and I. Riess. Kluwer, Dortrecht, Boston, London, 2000, pp. 389–397.
5. Lara, C., Pascual, M. J. and Durán, A., Glass and glass–ceramic sealants for solid oxide fuel cells. *Bol. Soc. Esp. Ceram. Vidrio.*, 2003, **42**, 133–143.
6. Fergus, J. W., Sealants for solid oxide fuel cells. *J. Power Sources*, **147**(1–2), 46–57.
7. Sohn, S. B., Choi, S. Y., Kim, G. H., Song, H. S. and Kim, G. D., Stable sealing glass for planar solid oxide fuel cells. *J. Non-Cryst. Solids*, 2002, **297**, 103–112.
8. Geasee, P., Doctoral Thesis, RWTH Aachen, Germany, 2003.
9. Stevenson, J., SOFC seals: materials status. In *SECA Core Technology Program-SOFC Seal Meeting*, 2003.
10. Yang, Z., Stevenson, J. W. and Meinhardt, K. D., Chemical interactions of barium–calcium–aluminosilicate-based sealing glasses with oxidation resistant alloys. *Solid State Ionics*, 2003, **160**, 213–225.
11. Haanappel, V. A. C., Shemet, V., Vinke, I. C., Gross, S. M., Koppitz, T., Menzler, N. H. *et al.*, Evaluation of the suitability of various glass sealant-alloy combinations under SOFC stack conditions. *J. Mater. Sci.*, 2005, **40**, 1583–1592.
12. Lara, C., Pascual, M. J., Prado, M. O. and Durán, A., Sintering of glasses in the system RO–Al_2O_3–BaO–SiO_2 (R = Ca, Mg, Zn) studied by hot-stage microscopy. *Solid State Ionics*, 2004, **170**, 201–208.
13. Lara, C., Pascual, M. J. and Durán, A., Glass-forming ability and thermal properties in the systems RO–BaO–SiO_2 (R = Mg, Zn). *J. Non-Cryst. Solids.*, 2004, **348**, 149–155.
14. Chou, Y. S. and Stevenson, J. W., Thermal cycling and degradation mechanism of compressive mica-based seals for solid oxide fuel cells. *J. Power Sources*, 2002, **112**, 376–383.
15. Chou, Y. S. and Stevenson, J. W., Mid-term stability of novel mica-based compressive seals for solid oxide fuel cells. *J. Power Sources*, 2003, **115**, 274–278.
16. Chou, Y. S. and Stevenson, J. W., Phologopite mica-based compressive seals for solid oxide fuel cells: effect of mica thickness. *J. Power Sources*, 2003, **124**, 473–478.
17. Bram, M., Reckers, S., Drinovac, P., Monch, J., Steinbrench, R. W., Buchkramer, H. P. *et al.*, Deformation behaviour and leakage test of alternative sealing material for SOFC stacks. *J. Power Sources*, 2004, **138**, 111–119.
18. Lara, C., Pascual, M. J., Keding, R. and Durán, A., Electrical behaviour of glass–ceramics in the systems RO–BaO–SiO_2 (R = Mg, Zn) for sealing SOFCs. *J. Power Sources*, in press [Epub ahead of print].
19. Rickert, H., *Electrochemistry of Solids. An Introduction*. Springer-Verlag, Berlin-Heidelberg, NY, 1982.
20. Liu, M. and Joshi, A., Characterization of mixed ionic-electronic conductors. In *Proceedings of 1st International Symposium on Ceramic Membranes*, ed. T. A. Ramanarayanan and H. L. Tuller. The Electrochemical Society, Pennington, NJ, 1991, pp. 231–246.
21. Kharton, V. V. and Marques, F. M. B., Interfacial effects in electrochemical cells for oxygen ionic conduction measurements. I. The e.m.f. method. *Solid State Ionics*, 2001, **140**, 381–394.
22. Gorelov, V. P., Transference number determination in ionic conductors by the e.m.f. method with active load. *Elektrokhimiya*, 1988, **24**, 1380–1381, in Russian.
23. Chase, M. W., NIST-JANAF thermochemical tables, fourth edition. *J. Phys. Chem. Ref. Data*, 1998, 1–1951, Monograph 9.
24. Shaula, A. L., Kharton, V. V. and Marques, F. M. B., Oxygen ionic and electronic transport in apatite-type $La_{10-x}(Si,Al)_6O_{26\pm\delta}$. *J. Solid State Chem.*, 2005, **178**, 2050–2061.
25. Schwartz, M. and Mackenzie, J. D., Ionic conductivity in calcium silicate glasses. *J. Am. Ceram. Soc.*, 1966, **49**, 582–585.
26. Evstropiev, K. K. and Petrovskii, G. T., Phenomenon of glass anionic conductivity. *Dokl. Akad. Nauk SSSR*, 1978, **241**, 1334–1336.
27. Desaglois, F., Follet-Houttemane, C. and Boivin, J. C., A new anionic conductive vitreous phase. *J. Mater. Chem.*, 2000, **10**, 1673–1677.
28. Jacob, S., Javornizky, J., Wolf, G. H. and Angel, C. A., Oxide ion conducting glasses-synthetic strategies based on liquid state and solid state routes. *Int. J. Inorg. Mater.*, 2001, **3**, 241–251.
29. Rao, K. J., Kumar, S. and Vinatier, P., Can any material form a glass? *Solid State Commun.*, 2004, **129**, 631–635.
30. Ishihara, T., Arikawa, H., Akbay, T., Nishiguchi, H. and Takita, Y., Non-stoichiometric $La_{2-x}GeO_{5-\delta}$ as a new fast oxide ionic conductor. *J. Am. Chem. Soc.*, 2001, **123**, 203–209.
31. Joubert, O., Magrez, A., Chesnaud, A., Caldes, M. T., Jayaraman, V., Piffard, Y. *et al.*, Structural and transport properties of a new class of oxide ion conductors. *Solid State Sci.*, 2002, **4**, 1413–1418.
32. Sakai, N., Yamaji, K., Horita, T., Yokokawa, H., Kawada, H. and Dokiya, M., Oxygen transport properties of $La_{1-x}Ca_xCrO_{3-\delta}$ as an interconnect material of a solid oxide fuel cell. *J. Electrochem. Soc.*, 2000, **147**, 3178–3182.
33. Tikhonovich, V. N., Zharkovskaya, O. M., Naumovich, E. N., Bashmakov, I. A., Kharton, V. V. and Vecher, A. A., Oxygen nonstoichiometry of $Sr(Co,Fe)O_{3-\delta}$-based perovskites. I. Coulometric titration of $SrCo_{0.85}Fe_{0.10}Cr_{0.05}O_{3-\delta}$ by the two-electrode technique. *Solid State Ionics*, 2003, **160**, 259–270.